NASA TM X-598

NASA TM X-598

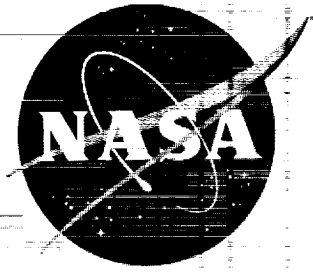

TECHNICAL MEMORANDUM

X-598

TRANSONIC AND SUPERSONIC FLUTTER TREND INVESTIGATION OF A VARIABLE-SWEEP WING

By John C. Stonesifer and Robert C. Goetz

Langley Research Center
Langley Air Force Base, Va.

NATIONAL AERONAUTICS AND SPACE ADMINISTRATION

WASHINGTON

October 1961

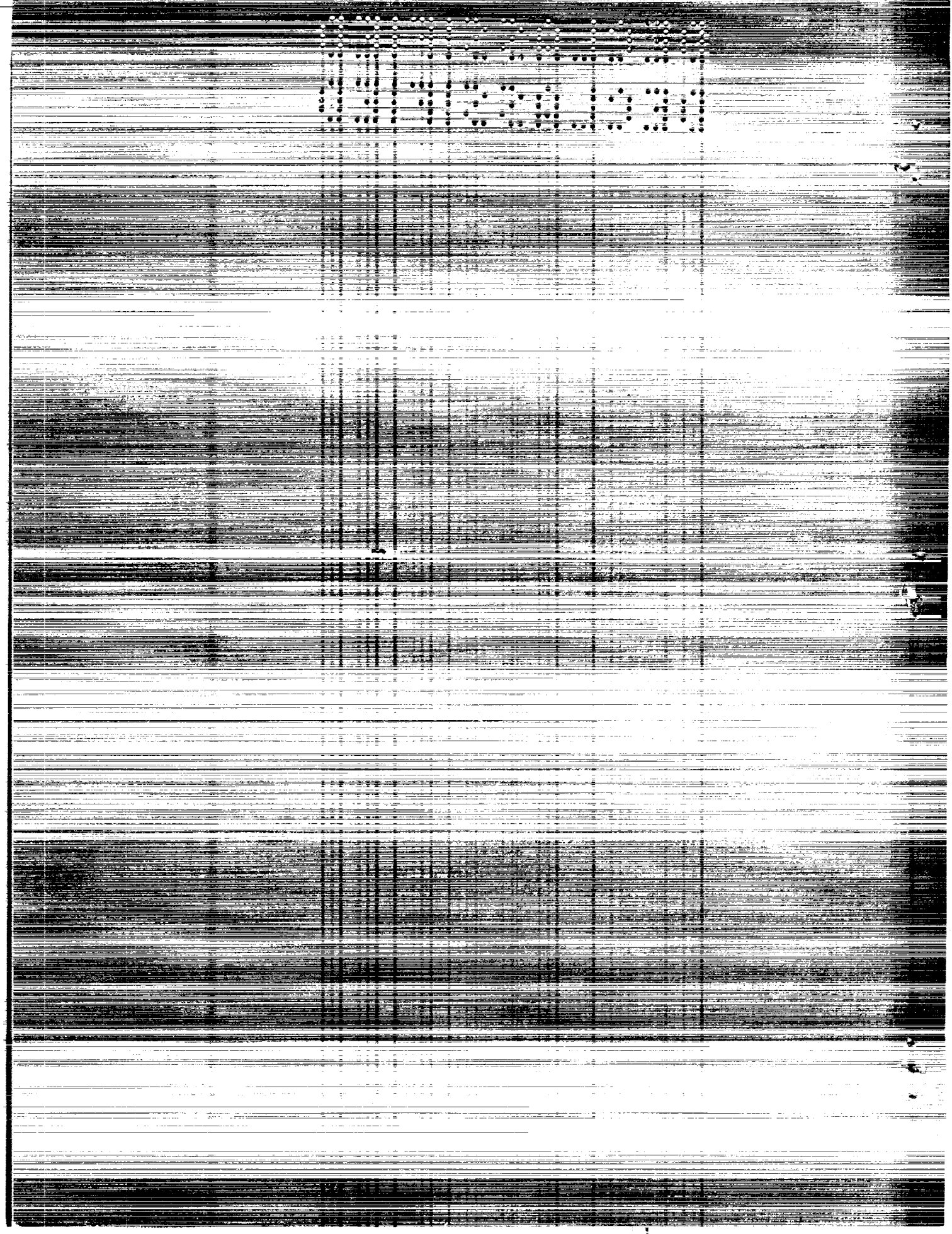

NATIONAL AERONAUTICS AND SPACE ADMINISTRATION

TECHNICAL MEMORANDUM X-598

TRANSONIC AND SUPERSONIC FLUTTER TREND INVESTIGATION OF A VARIABLE-SWEEP WING*

By John C. Stonesifer and Robert C. Goetz

SUMMARY

An exploratory flutter trend investigation of a tapered variable-sweep wing design has been made in the Langley transonic blowdown tunnel and in the Langley 9- by 18-inch supersonic aeroelasticity tunnel at Mach numbers from about 0.50 to 2.55. Three planforms were tested in order to represent the variable-sweep wing in three sweep positions. These planforms had inboard panels which were swept back 60° at the leading edge, whereas the outboard panels were swept back 25°, 60°, and 75° at the leading edge. The assumed pivot point was located on the quarter chord of the outboard panel at about 25-percent exposed semispan of the 60° configuration. The models were of simple construction and did not simulate joint flexibility.

The results at transonic Mach numbers indicate a favorable increase in flutter speeds as the wing sweep angle is increased. At supersonic Mach numbers the 25° sweptback wing exhibited the highest flutter speeds. An appreciable difference between data obtained in the two tunnels is attributed to the different values of mass-density ratio obtained at flutter in the two test facilities.

INTRODUCTION

An airplane combining the characteristics of low-speed efficiency and supersonic-cruise ability would be useful in many operations. In general, however, the dual requirements of low-speed efficiency and supersonic flight are not compatible. In order to accomplish this mission, one would have to compromise the performance of the aircraft or be able to alter its configuration in flight. One method of alteration incorporates variation of the wing sweep by rotating the outer wing panels while the inboard panels remain fixed.

*Title, Unclassified.

The use of a variable-sweep configuration, being a new concept, necessitates the need for information that would permit the prediction of its flutter trend characteristics. The purpose of this report is to present the data obtained in an exploratory investigation of the flutter characteristics of a variable-sweep wing in three fixed-sweep positions.

The data were obtained in the Langley transonic blowdown tunnel and in the Langley 9- by 18-inch supersonic aeroelasticity tunnel at Mach numbers from about 0.50 to 2.55. Three planforms were tested in order to represent the variable-sweep wing in three sweep positions. These planforms had inboard panels which were swept back 60° at the leading edge, whereas the outboard panels were swept back 25°, 60°, and 75° at the leading edge. The assumed pivot point was located on the quarter chord of the outboard panel at about 25-percent exposed semispan of the 60° configuration. The models were of simple construction and did not simulate joint flexibility.

It is recognized that reliable flutter information for a given design would require a more realistic model which simulates the design stiffness, mass distribution, and joint flexibility; however, it is believed that the present data will be useful for preliminary considerations.

SYMBOLS

a	speed of sound, ft/sec
b	structural streamwise semichord at root, ft
b_y	streamwise semichord at station y, ft
f_f	flutter frequency, cps
$f_{h,i}$	measured bending frequencies (i = 1, 2, 3), cps
f_α	measured first torsion frequency, cps
l	exposed semispan, ft
m	mass of one exposed wing panel, slugs
M	Mach number
q	dynamic pressure, lb/sq ft

S exposed area of one wing panel, sq ft

V stream velocity, ft/sec

y distance from root chord spanwise, ft

Λ sweepback of leading edge of outboard part of wing, deg

μ mass-density ratio, nondimensional, $\dfrac{m}{\pi\rho \int_0^l b_y^2 dy}$

ρ air density, slugs/cu ft

ω_α measured first torsion frequency, $2\pi f_\alpha$, radians/sec

Subscripts:

A pertaining to average values for left and right panels of construction A models having the same planform

adj value adjusted to what it would be for construction A

min minimum adjusted value of 25° configuration

MODELS

The three planforms shown in figure 1 were investigated. Each planform had NACA 65A005.5 airfoil sections normal to the leading edge and an inboard part of the wing swept back 60° along the leading edge. The outboard panels of the different planforms were swept back 25°, 60°, and 75° along the leading edge.

These three configurations simulate planforms that would result as the outer panels are rotated to vary the sweep angle. The assumed pivot point was located on the quarter chord of the outboard panel at about 25-percent semispan of the 60° configuration. The division between the inboard and outboard panels is shown in figure 1. In an airplane with a variable-sweep wing, provision must be made to enclose that part of the wing which disappears as the sweep of the outer panels is increased. Depending on how this is accomplished, the wing trailing edge might not be a straight continuous line near the root as it was for the present models. (See fig. 1.) Therefore, in order to provide some structural consistency for the present models, the structural root chord was arbitrarily made the same (5.55 inches as shown in fig. 1) for all three planforms by cutting the root chords at the trailing edges for the 25° and 75° swept wings.

The models were machined from solid Formica. In order to obtain flutter throughout the dynamic-pressure range available in the tunnels, it was necessary to reduce the stiffnesses of some of the models. The stiffness reductions were accomplished by cutting a pattern of holes and slots through the outboard panels normal to the chord plane. The inboard part of the wing was not drilled or slotted for it is believed that for an airplane with a variable-sweep wing this fixed inboard wing area will have to be comparatively stiff to support the sweep mechanism and carry the loads. For models with holes and slots, the wings were wrapped with a layer of silk which was doped and painted to provide a leakproof surface. The solid models are referred to herein as construction A, and models with progressively larger holes and longer slots, and thus progressively reduced stiffnesses, are referred to as constructions B, C, D, and E. A photograph of a drilled and slotted semispan model (construction E) is shown in figure 2.

Physical characteristics of all wing panels tested are listed in table I. Both full-span and semispan sting-mounted models were used in the transonic tests. Wall-mounted semispan models only were used in the supersonic tests. In the transonic tests, although the boundary conditions for the full-span and semispan models are different, experience with these models and past experience with similar models has shown that the flutter speed is not affected. In many cases, the same model was used for several flutter points before it was damaged or destroyed. A model used in more than one run was checked for structural damage by visual inspection and by comparing natural vibration frequencies of the model obtained before and after each run.

Table I also presents the measured natural vibration frequencies and the ratios of the first and second bending frequencies to the first torsion frequency for the various models investigated. For a given planform, the frequency ratios are shown to be relatively constant as the method of construction is changed. The natural vibration node lines for the various methods of construction also remained relatively constant for a given planform and are shown in figure 3. For the determination of the natural frequencies and node lines, each model was clamped to a steel bench in such a manner that each wing panel could be considered as cantilevered from the root-clamping block. (See fig. 2.) An acoustical shaker was used to excite the models. Sand grains sprinkled on the wing surface were used to identify the node lines.

APPARATUS AND TESTS

Transonic Tests

The tests were conducted in the Langley transonic blowdown tunnel for the Mach number range from 0.50 to 1.30. The transonic blowdown

tunnel has an octagonal test section with a slot in each corner and measures $26\frac{1}{4}$ inches between flats. During operation of the tunnel a preselected Mach number is set by means of a variable orifice downstream of the test section. This Mach number is held approximately constant after the orifice is choked, while the stagnation pressure, and thus the density, is increased. However, the area of the orifice may also be varied during a run as the stagnation pressure is increased or held constant so that various operating paths of Mach number and density may be followed. Both methods of operation were used in the present investigation and are illustrated in figure 4.

The static-density range is approximately 0.001 to 0.012 slug per cubic foot. It should be noted that, because of the expansion of the air in the reservoir during a run, the stagnation temperature continually decreases so that the test-section velocity is not uniquely defined by the Mach number. Additional details of the tunnel are contained in reference 1.

The models were mounted on a $1\frac{1}{2}$-inch-diameter sting which formed a fuselage that extended upstream into the subsonic-flow region of the tunnel. This arrangement prevented the formation of shock waves from the fuselage nose which might reflect from the tunnel walls onto the model. The 65-pound sting was considered to form a rigid mount for the models since the mass of the complete support system was very large compared with the mass of a model. The fundamental frequency of the support system was approximately 14.5 cycles per second.

An optical system displayed an image of the model on a ground-glass screen during the runs. When flutter was observed, the airflow was quickly stopped in an effort to save the model from destruction by flutter.

Supersonic Tests

The Langley 9- by 18-inch supersonic aeroelasticity tunnel is a conventional fixed-nozzle blowdown-type wind tunnel exhausting into a vacuum sphere from a pressure reservoir. The nozzles used gave Mach numbers of 1.30, 1.64, 2.00, and 2.55. At each Mach number, the test-section density varies continuously to a controlled maximum density and then decreases. Maximum test-section conditions are depicted in the tunnel performance curves shown in figure 5.

For each Mach number in the supersonic tunnel, the test procedure was essentially the same. The sphere to which the tunnel exhausts and the test section were pumped down to a pressure of approximately

2 pounds per square inch absolute. The control valve upstream of the test section was then opened and the test-section density was allowed to increase until flutter was observed or the maximum density was reached.

The models were cantilever-mounted in a mounting block. The mounting block, in turn, was attached to the head of a ram that was used to retract the models through one side of the tunnel in an effort to save the models from destruction after the onset of flutter. The models were viewed through a window in the opposite side of the test section.

Instrumentation

Resistance-type, electrical strain gages were mounted on the surface of all models near the root to establish the occurrence of flutter and to indicate the frequency of the flutter oscillation. These gages were oriented so as to indicate as nearly as possible the separate bending and torsional strains of the wings. A multichannel recording oscillograph was employed to record the time history of the strain-gage signals and the tunnel conditions during the runs. High-speed motion pictures furnished a visual record of the model motions.

RESULTS AND DISCUSSION

The basic results of this investigation are presented in table II. The first three columns identify the models as to construction, model number, and full span or semispan. Two full-span models (models 10 and 11) were tested also as semispan models after the right panels were damaged by flutter. The column labeled "wing-panel behavior" contains a code system defined at the bottom of table II to describe each data point. The low damping behavior indicated by the code letter D is characterized by a period of intermittent bursts of sinusoidal oscillations which sometimes obscured the exact start of flutter. Flutter frequencies as obtained from the strain-gage traces are given in the column labeled f_f. In most cases, the flutter appeared to be of a limited amplitude type.

The flutter and no-flutter points from table II are plotted in figure 6 in the form of the nondimensional flutter-speed index $\frac{V}{b\omega_\alpha\sqrt{\mu}}$ as a function of Mach number. It should be noted that for a given planform

$$\frac{V}{b\omega_\alpha\sqrt{\mu}} \propto \sqrt{\frac{qb}{m\omega_\alpha^2}}$$

Thus the flutter-speed index is adjusted for variations of the dynamic pressure by the mass and torsional-frequency characteristics of the models.

For a variety of configurations, past experience has shown that the conventional transonic variation of flutter-speed index with Mach number is an almost constant value to a point near $M = 1$ and then, after a slight decrease, increases with Mach number. Figure 6 indicates that all three planforms exhibit this conventional variation, but to a different degree for each planform. However, the supersonic flutter boundary for each planform exhibits somewhat unusual behavior in that the boundaries obtained in the two wind tunnels do not fair together but show a definite difference at $M = 1.3$, a Mach number common to both facilities. Each flutter boundary as shown is composed of two segments. The two segments when considered separately do, however, resemble conventional flutter trends.

It should be noted that, of the several methods of model construction, only construction E models could be fluttered in the supersonic tunnel. A comparison of construction E models with those of other constructions showed there was no shift in model center-of-gravity position or noticeable change in frequency ratio or node line characteristics to cause the difference in the data. A further look at other model properties and test conditions indicates that the difference in the data is most likely due to the different values of mass-density ratio obtained at flutter in the two tunnels. A comparison of density ranges of the two tunnels is presented in figure 7. For these densities, the mass-density ratio at flutter for models tested in the transonic tunnel ranged from about 8 to 30 as compared with 36 to 56 in the supersonic tunnel.

Some support for attributing this difference in the data to density difference between the two tunnels is offered by figure 8. In this figure, data from reference 2 are combined with some unpublished test results. These combined data show the variation of flutter-speed index with Mach number for an aspect-ratio-4, taper-ratio-0.2, 45° sweptback wing. As shown, there also is a difference in the data at a Mach number of 1.3. These data were obtained in the same two tunnels used in the present investigation. In addition to the experimental data, some calculated flutter boundaries for this same wing are presented in figure 8. These calculations (unpublished), based on the method of reference 3 and made by Yates, agree well with the experimental data and support the conclusion that a difference such as occurred in the present investigation can result solely from a variation in the density. The data of reference 4

also indicate that appreciable scatter in flutter data results if density changes are large.

The flutter boundary curves in figure 9 show the relative flutter susceptibility of the three planforms over the Mach number range of the investigation. In this figure the dynamic pressures for flutter for a given planform of the different constructions, B, C, D, and E, are adjusted to what would result for construction A and then normalized to the minimum adjusted dynamic pressure of the 25° configuration. This adjusted dynamic pressure is obtained from the following simple relationship between the flutter-speed indices for models of a given planform but of different construction:

$$\left(\frac{V}{b\omega_\alpha\sqrt{\mu}}\right)_A^2 = \left(\frac{V}{b\omega_\alpha\sqrt{\mu}}\right)_j^2$$

(where A represents construction A and j represents constructions B, C, D, and E). This equation thus yields

$$q_{adj} = \left(\frac{b^2\omega_\alpha{}^2 m}{2\pi\int_0^l b_y{}^2 dy}\right)_A \left(\frac{V}{b\omega_\alpha\sqrt{\mu}}\right)_j^2$$

At low speeds the 60° and 75° sweptback wings require dynamic pressures for flutter, respectively, 1.6 and 2.4 times that required for the 25° sweptback wing. It may be noted that the transonic dip in dynamic pressure for flutter occurs at progressively higher Mach numbers and is less severe as the sweepback angle is increased. All three planforms indicate a favorable trend in Mach number effect following the transonic dips. It should be remembered, however, that for the present models, as the sweep angle was increased, certain changes in stiffness (and torsion frequency, see table I) were obtained and this change in stiffness, of course, influences the relative flutter susceptibility of the different planforms. If on the variable-sweep wing a different change in stiffness with sweep angle were obtained, as might be expected with a pivot joint, the relative flutter susceptibility would be different.

Also shown in figure 9 are two curves of constant altitude. The actual altitudes simulated by these curves, of course, depend upon the scale factor required to relate the dynamic pressure for the model to the dynamic pressure for the airplane. However, the altitude lines shown with the flutter boundaries emphasize that the relative flutter

susceptibility of the different sweep positions would have to be considered when programing the wing-sweep changes for a particular flight plan.

CONCLUSIONS

The results of a flutter trend investigation in the Langley transonic blowdown tunnel and in the Langley 9- by 18-inch supersonic aeroelasticity tunnel of very simple models of a tapered variable-sweep wing design indicate the following conclusions:

1. At low speeds the 60° and 75° sweptback wings required, respectively, 1.6 and 2.4 times the dynamic pressure of the 25° sweptback wing for flutter.

2. The transonic dip in dynamic pressure for flutter occurred at progressively higher Mach numbers and was less severe as the sweepback angle was increased.

3. A favorable trend in Mach number effect for all three planforms followed the transonic dips.

4. A difference in the data from the two tunnels was obtained and indicates that careful consideration should be given to the mass-density ratio as a design factor when testing flutter models in different tunnels.

Langley Research Center,
National Aeronautics and Space Administration,
Langley Air Force Base, Va., July 20, 1961.

REFERENCES

1. Unangst, John R., and Jones, George W., Jr.: Some Effects of Sweep and Aspect Ratio on the Transonic Flutter Characteristics of a Series of Thin Cantilever Wings Having a Taper Ratio of 0.6. NACA RM L55I13a, 1956.

2. Unangst, John R.: Transonic Flutter Characteristics of an Aspect-Ratio-4, 45° Sweptback, Taper-Ratio-0.2 Planform. NASA TM X-136, 1959.

3. Yates, E. Carson, Jr.: Calculation of Flutter Characteristics for Finite-Span Swept or Unswept Wings at Subsonic and Supersonic Speeds by a Modified Strip Analysis. NACA RM L57L10, 1958.

4. Yates, E. Carson, Jr.: Some Effects of Variations in Density and Aerodynamic Parameters on the Calculated Flutter Characteristics of Finite-Span Swept and Unswept Wings at Subsonic and Supersonic Speeds. NASA TM X-182, 1960.

TABLE I.- PHYSICAL CHARACTERISTICS OF MODELS INVESTIGATED

Type of construction	Model	Configuration	Panel	m, slugs	$f_{h,1}$, cps	$f_{h,2}$, cps	f_{α}, cps	$f_{h,3}$, cps	$f_{h,1}/f_{\alpha}$	$f_{h,2}/f_{\alpha}$
$\Lambda = 25^{\circ}$; S = 0.1191 sq ft										
A	1	Full span	Left	0.00276	91	303	675	690	0.13	0.45
A	1	Full span	Right	.00276	90	314	690	717	.13	.46
C	2	Full span	Left	.00252	75	260	515	605	.15	.50
C	2	Full span	Right	.00252	76	268	522	622	.15	.51
C	3	Semispan	-----	.00269	81	294	510	665	.16	.58
E	4	Semispan	-----	.00240	62	238	460	553	.13	.52
E	5	Semispan	-----	.00231	56	225	447	523	.13	.50
E	6	Semispan	-----	.00231	59	230	470	534	.13	.49
E	7	Semispan	-----	.00242	58	240	455	567	.13	.53
E	8	Semispan	-----	.00239	61	242	460	560	.13	.53
$\Lambda = 60^{\circ}$; S = 0.1103 sq ft										
A	9	Full span	Left	0.00290	120	375	778	920	0.15	0.48
A	9	Full span	Right	.00290	121	370	750	890	.16	.49
B	10	Full span	Left	.00281	100	328	645	758	.16	.51
B	10	Full span	Right	.00281	100	330	640	765	.16	.52
C	11	Full span	Left	.00250	97	310	600	699	.16	.52
C	11	Full span	Right	.00248	96	302	600	-----	.16	.50
E	12	Semispan	-----	.00266	75	260	500	600	.15	.52
E	13	Semispan	-----	.00259	74	263	514	600	.14	.51
E	14	Semispan	-----	.00238	69	250	480	575	.14	.52
E	15	Semispan	-----	.00257	74	271	500	630	.15	.54
$\Lambda = 75^{\circ}$; S = 0.1068 sq ft										
A	16	Full span	Left	0.00287	145	433	791	1,030	0.18	0.55
A	16	Full span	Right	.00287	139	431	796	1,050	.17	.54
C	17	Semispan	-----	.00248	111	375	645	833	.17	.58
D	18	Semispan	-----	.00259	101	360	615	800	.16	.59
E	19	Semispan	-----	.00234	76	264	527	625	.14	.50
E	20	Semispan	-----	.00229	79	300	522	700	.15	.57
E	21	Semispan	-----	.00234	85	300	550	690	.15	.55
E	22	Semispan	-----	.00237	85	308	550	700	.15	.56

TABLE II.- COMPILATION OF EXPERIMENTAL RESULTS

Type of construction	Model	Configuration	Run	Point	Wing-panel behavior (a)	f_f, cps for -		M	q, lb/sq ft	V, ft/sec	ρ, slugs/cu ft	a, ft/sec	μ	$V/b\omega_\alpha\sqrt{\mu}$
						Left panel	Right panel							
$\Lambda = 25°$														
A	1	Full span	1	1	Q	---	---	0.683	768	736	0.00282	1,078	39.93	0.118
A	1	Full span	2	1	F	283	283	.806	1,655	833	.00476	1,034	23.67	.173
A	1	Full span	3	1	Q	---	---	1.298	4,290	1,168	.00629	900	11.58	.373
A	1	Full span	4	1	Q	---	---	1.063	3,987	989	.00813	931	13.86	.268
A	1	Full span	5	1	Q	---	---	.977	3,563	931	.00820	953	13.74	.254
A	1	Full span	6	1	F	293	300	.769	1,745	806	.00537	1,047	20.99	.177
A	1	Full span	7	1	D	---	---	.833	1,354	874	.00354	1,050	31.83	.157
A	1	Full span	7	2	F	253	253	.843	1,480	881	.00381	1,046	29.56	.164
A	1	Full span	8	1	F	412	384	.951	3,486	938	.00791	987	14.24	.251
A	1	Full span	9	1	F	270	270	.915	2,038	934	.00467	1,020	24.11	.192
A	1	Full span	10	1	F	333	333	.945	2,847	946	.00635	1,001	17.74	.227
A	1	Full span	11	1	Q	---	---	.706	2,244	695	.00926	985	12.17	.201
A	1	Full span	12	1	F	360	360	.632	2,098	667	.00942	1,056	11.96	.195
A	1	Full span	13	1	F	325	325	.708	2,043	732	.00760	1,034	14.83	.192
C	2	Full span	14	1	F	317	317	.608	1,024	656	.00475	1,079	21.64	.187
C	3	Semispan	15	1	Q	---	---	.578	1,197	610	.00641	1,056	17.12	.199
C	3	Semispan	16	1	F	325	---	.575	1,187	608	.00641	1,058	17.12	.199
C	3	Semispan	17	1	F	333	---	.521	1,217	552	.00799	1,059	13.74	.201
E	4	Semispan	[b]18	1	Q	---	---	2.000	2,623	1,712	.00179	856	54.70	.347
E	5	Semispan	[b]19	1	Q	---	---	2.000	3,357	1,716	.00228	858	41.35	.412
E	6	Semispan	[b]20	1	F	300	---	1.640	2,546	1,561	.00209	952	45.12	.340
E	7	Semispan	[b]21	1	F	275	---	1.300	1,921	1,287	.00232	990	42.56	.299
E	8	Semispan	[b]22	1	Q	---	---	2.550	2,808	1,948	.00148	764	65.95	.360
$\Lambda = 60°$														
A	9	Full span	23	1	Q	---	---	1.297	4,340	1,182	0.00620	911	16.95	0.259
A	9	Full span	24	1	Q	---	---	.822	3,118	819	.00928	996	11.32	.219
A	9	Full span	25	1	Q	---	---	.939	3,524	904	.00861	962	12.21	.233
B	10	Full span	26	1	Q	---	---	1.285	4,271	1,158	.00637	901	15.99	.311
B	10	Full span	27	1	F	300	300	.980	2,210	1,002	.00440	1,022	23.14	.223
B	10	Full span	28	1	F	328	328	.833	2,491	848	.00692	1,018	14.71	.237
B	10	Full span	29	1	F	335	335	1.054	2,909	1,038	.00540	985	18.59	.256
B	10	Left panel	30	1	F	300	---	.934	2,557	928	.00593	994	17.17	.239
B	10	Left panel	31	1	F	350	---	1.125	3,691	1,067	.00647	949	15.74	.287
B	10	Left panel	32	1	F	333	---	.805	2,701	793	.00858	985	11.86	.246
B	10	Left panel	33	1	D	---	---	.995	2,128	1,004	.00421	1,009	24.19	.218
B	10	Left panel	33	2	Q	---	---	1.015	2,431	1,020	.00467	1,005	21.79	.233
B	10	Left panel	34	1	D	---	---	.991	2,111	1,002	.00420	1,011	24.25	.217
B	10	Left panel	34	2	F	300	---	1.008	2,406	1,012	.00470	1,004	21.66	.232
B	10	Left panel	35	1	F	386	---	1.174	4,291	1,094	.00716	932	14.22	.310
C	11	Full span	36	1	Q	---	---	1.300	4,306	1,193	.00605	918	14.91	.355
C	11	Full span	37	1	F	(c)	280	.965	1,665	975	.00350	1,010	25.67	.221
C	11	Left panel	38	1	D	---	---	.820	2,124	842	.00599	1,026	15.11	.248
C	11	Left panel	38	2	F	340	---	.804	2,239	823	.00660	1,024	13.72	.255
C	11	Left panel	39	1	Q	---	---	1.171	4,189	1,085	.00711	926	12.74	.349
C	11	Left panel	40	1	F	318	---	.843	1,922	904	.00470	1,072	19.27	.236

[a]Q denotes maximum dynamic pressure and no flutter; D denotes start of low damping conditions; and F denotes flutter.

[b]Designates a run made in supersonic aeroelasticity tunnel; all others made in transonic blowdown tunnel.

[c]Tunnel was shut down before left wing fluttered.

TABLE II.- COMPILATION OF EXPERIMENTAL RESULTS - Concluded

Type of construction	Model	Configuration	Run	Point	Wing-panel behavior (a)	f_f, cps for -		M	q, lb/sq ft	V, ft/sec	ρ, slugs/cu ft	a, ft/sec	μ	$V/b\omega_\alpha\sqrt{\mu}$
						Left panel	Right panel							
Λ = 60°														
C	11	Left panel	41	1	F	317	---	0.863	1,895	924	0.00444	1,070	20.41	0.235
C	11	Left panel	42	1	F	325	---	1.040	2,212	1,076	.00382	1,035	23.72	.254
C	11	Left panel	43	1	F	310	---	.915	1,817	963	.00391	1,053	23.17	.229
C	11	Left panel	44	1	D	---	---	.931	1,678	973	.00354	1,045	25.58	.221
C	11	Left panel	44	2	F	305	---	.965	1,981	1,005	.00392	1,042	23.11	.240
C	11	Left panel	45	1	D	---	---	1.112	2,720	1,136	.00421	1,022	21.52	.281
C	11	Left panel	45	2	F	350	---	1.133	2,959	1,159	.00440	1,023	20.59	.293
C	11	Left panel	46	1	F	308	---	.696	1,837	759	.00636	1,091	14.24	.231
C	11	Left panel	47	1	F	308	---	.726	1,920	799	.00601	1,100	15.07	.236
C	11	Left panel	48	1	F	350	---	1.105	2,820	1,169	.00412	1,058	21.98	.286
C	11	Left panel	49	1	F	312	---	1.035	2,029	1,072	.00352	1,036	25.72	.243
C	11	Left panel	50	1	F	300	---	.998	1,940	1,025	.00368	1,028	24.61	.238
C	11	Left panel	51	1	F	283	---	.940	1,686	976	.00354	1,037	25.58	.221
C	11	Left panel	52	1	D	---	---	.921	1,606	956	.00351	1,038	25.80	.216
C	11	Left panel	52	2	F	320	---	.983	2,004	1,013	.00390	1,030	23.22	.241
C	11	Left panel	53	1	F	325	---	.785	1,870	839	.00530	1,069	17.09	.233
C	11	Left panel	54	1	Q	---	---	1.302	3,470	1,366	.00371	1,050	24.42	.318
C	11	Left panel	55	1	F	388	---	1.158	3,398	1,217	.00459	1,051	19.74	.314
C	11	Left panel	56	1	F	420	---	1.178	4,049	1,193	.00569	1,013	15.92	.343
C	11	Left panel	[b]57	1	Q	---	---	2.000	3,461	1,750	.00226	875	40.08	.308
E	12	Semispan	[b]58	1	F	335	---	2.000	3,075	1,732	.00205	866	47.03	.348
E	13	Semispan	[b]59	1	F	300	---	1.640	2,069	1,574	.00167	960	56.22	.281
E	14	Semispan	[b]60	1	F	280	---	1.300	1,400	1,287	.00169	990	50.99	.259
E	15	Semispan	[b]61	1	Q	---	---	2.550	3,066	2,015	.00151	790	61.62	.353
Λ = 75°														
A	16	Full span	62	1	Q	---	---	1.241	4,077	1,132	0.00635	912	13.14	0.271
A	16	Full span	63	1	Q	---	---	.906	3,015	895	.00752	988	11.10	.233
A	16	Full span	64	1	Q	---	---	1.102	4,003	1,024	.00763	929	10.94	.269
A	16	Full span	65	1	Q	---	---	1.136	4,087	1,063	.00722	936	11.54	.272
C	17	Semispan	66	1	F	365	---	.959	3,044	961	.00658	1,002	10.96	.310
C	17	Semispan	67	1	F	360	---	1.189	3,468	1,146	.00527	964	13.68	.331
C	17	Semispan	68	1	F	360	---	1.089	3,262	1,066	.00573	979	12.58	.321
C	17	Semispan	69	1	Q	---	---	.839	2,900	817	.00867	974	8.32	.303
D	18	Semispan	70	1	D	---	---	1.287	3,558	1,225	.00473	952	15.91	.344
D	18	Semispan	70	2	F	360	---	1.286	3,648	1,222	.00488	950	15.42	.349
D	18	Semispan	71	1	F	344	---	.789	2,850	794	.00904	1,006	8.33	.308
D	18	Semispan	72	1	F	333	---	1.035	2,884	1,035	.00538	1,000	13.99	.310
D	18	Semispan	73	1	F	325	---	1.037	2,786	1,084	.00474	1,045	15.88	.305
D	18	Semispan	74	1	F	312	---	1.078	2,651	1,111	.00429	1,031	17.55	.297
E	19	Semispan	[b]75	1	Q	---	---	2.000	3,187	1,714	.00217	857	34.71	.326
E	20	Semispan	[b]76	1	F	345	---	2.000	2,837	1,728	.00190	864	35.81	.377
E	21	Semispan	[b]77	1	F	291	---	1.640	2,191	1,555	.00182	948	36.58	.340
E	22	Semispan	[b]78	1	F	285	---	1.300	1,570	1,296	.00187	997	36.35	.269
E	22	Semispan	[b]79	1	Q	---	---	2.550	3,066	2,015	.00151	790	45.62	.370

[a] Q denotes maximum dynamic pressure and no flutter; D denotes start of low damping conditions; and F denotes flutter.

[b] Designates a run made in supersonic aeroelasticity tunnel; all others made in transonic blowdown tunnel.

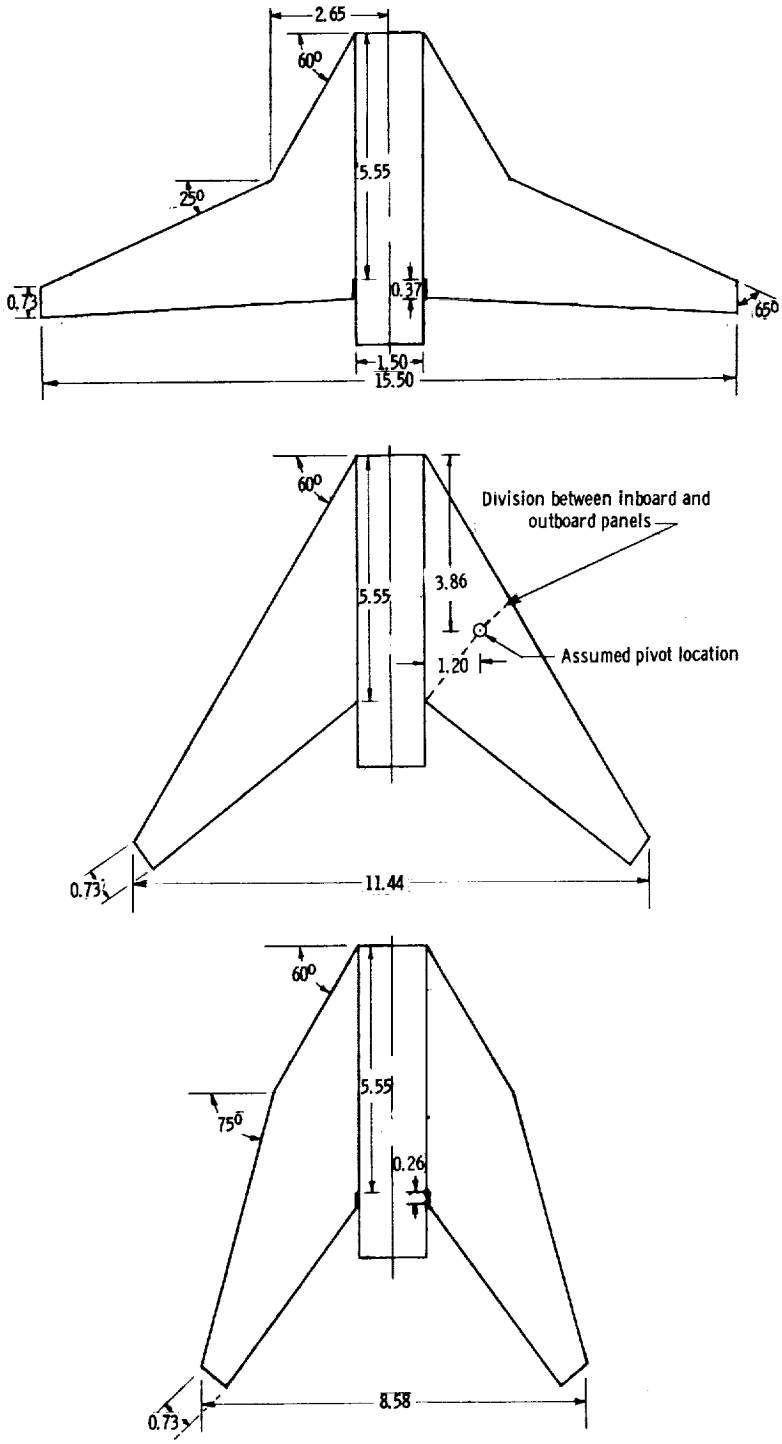

Figure 1.- Planforms of models investigated. All dimensions are in inches.

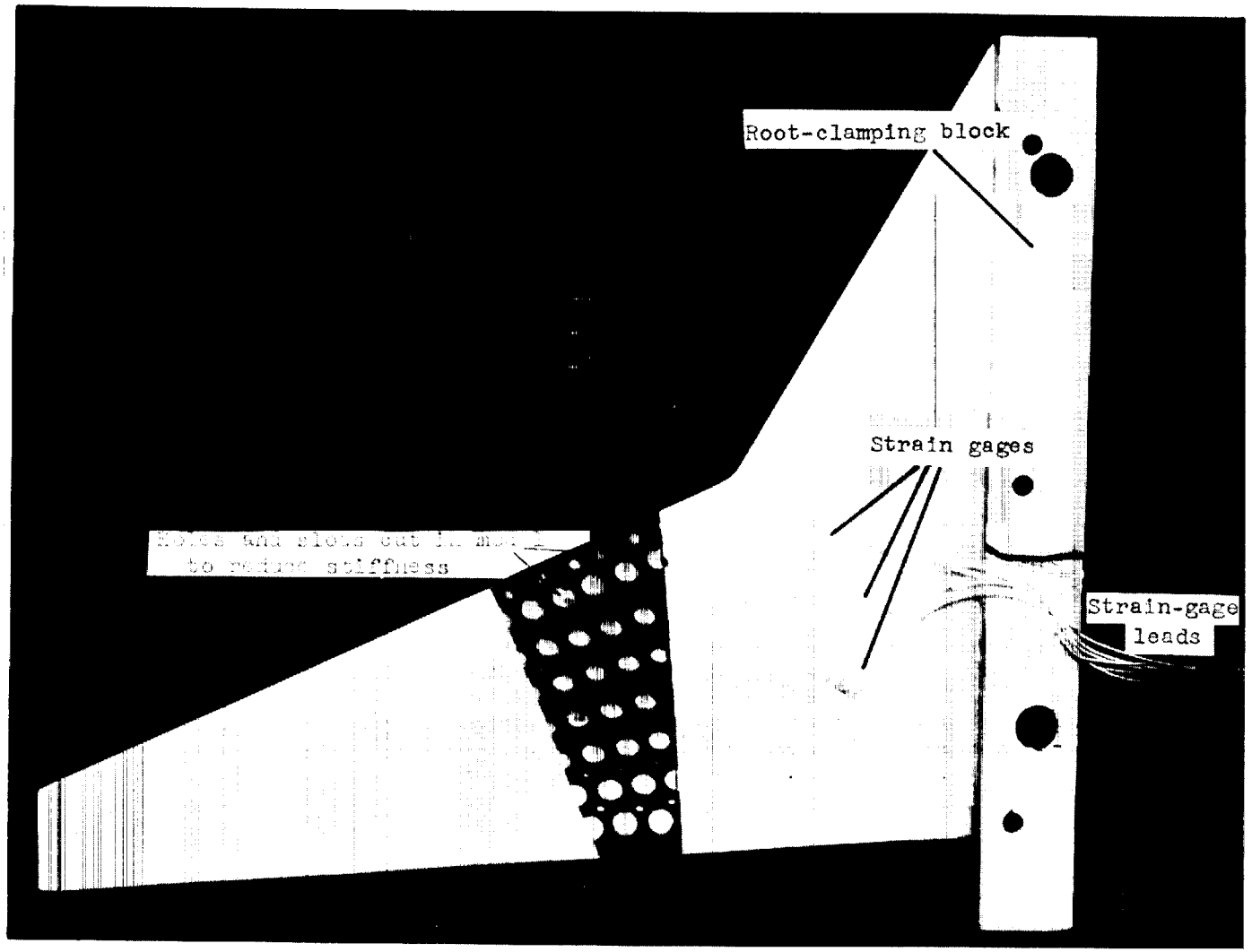

L-60-5487.1

Figure 2.- Photograph of a model (construction E) with portion of silk covering removed.

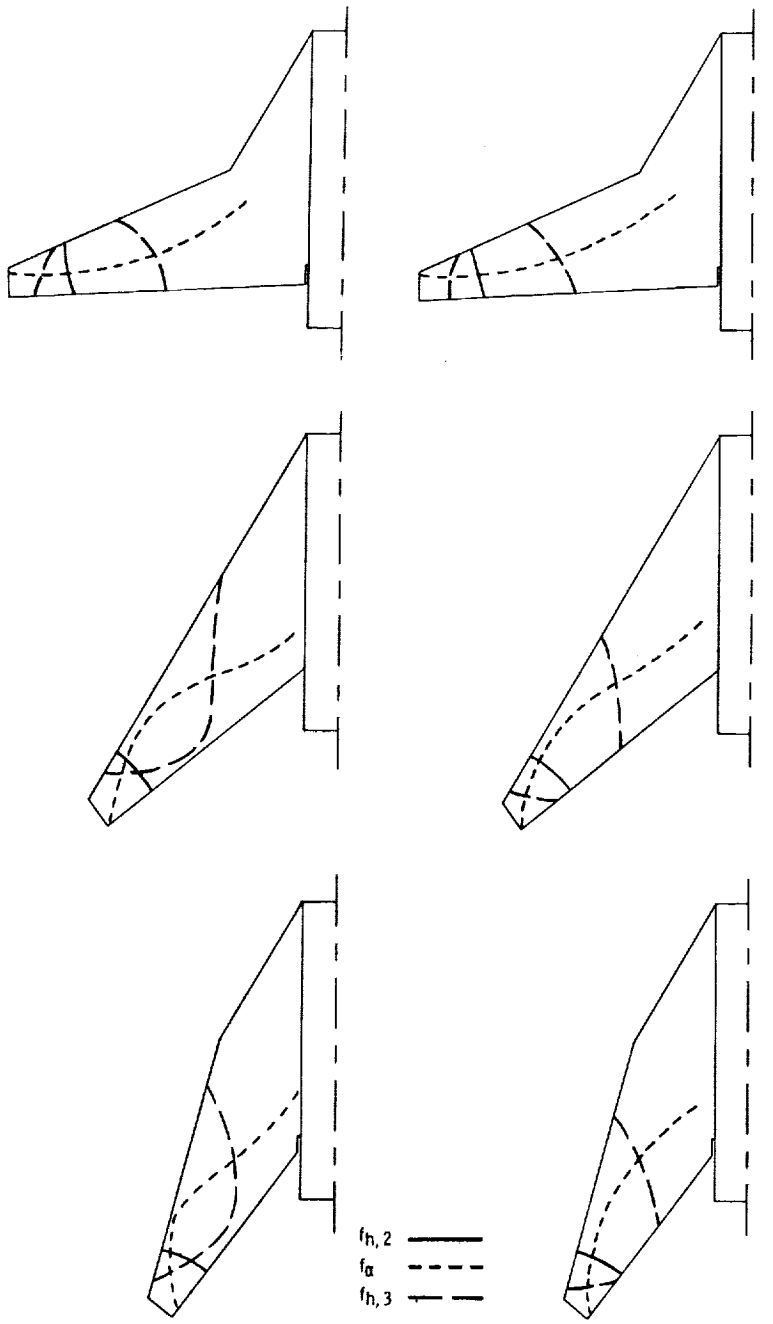

(a) For construction A.

(b) For constructions B, C, D, and E.

Figure 3.- Typical node lines for models investigated.

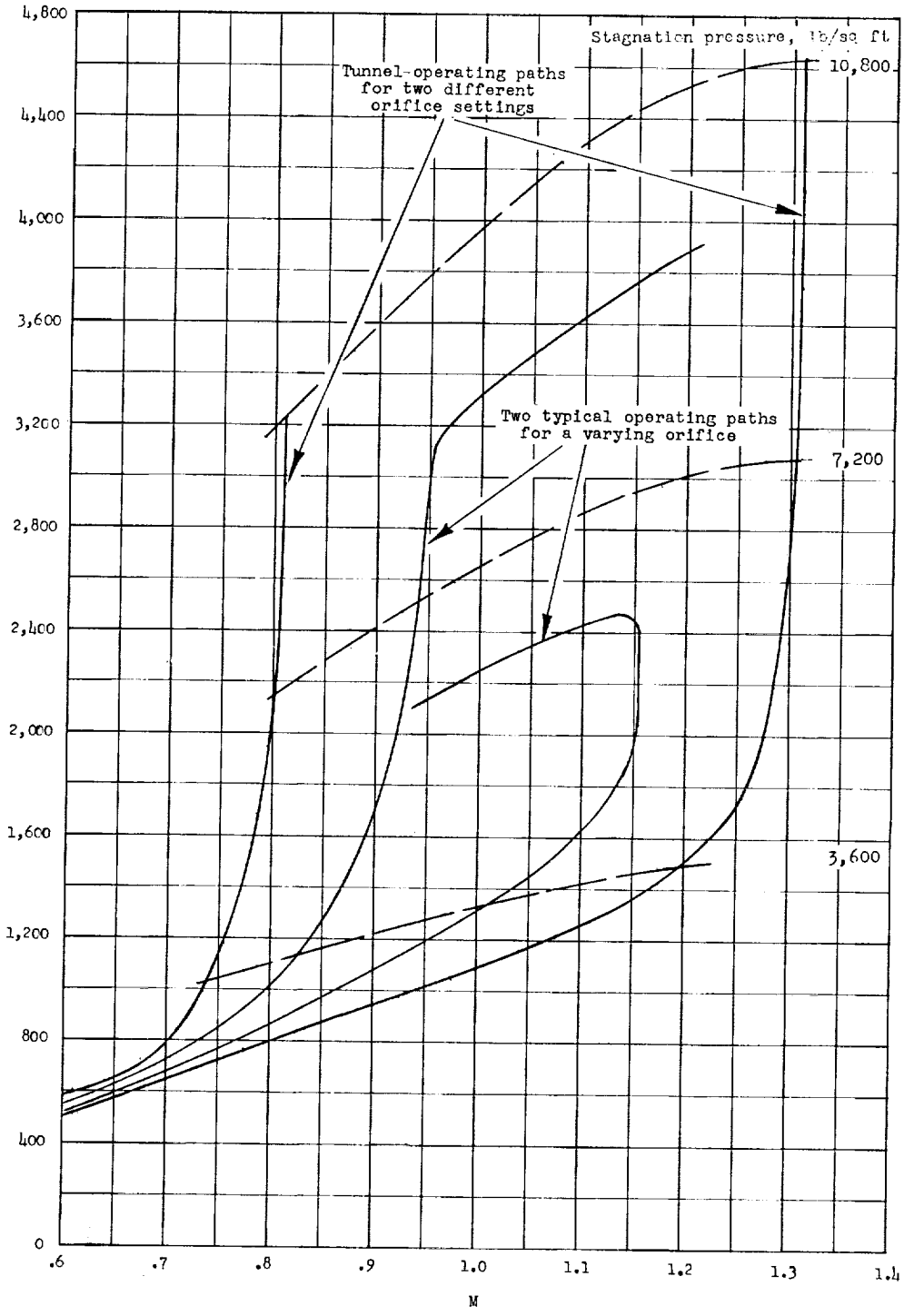

Figure 4.- Operating characteristics of the Langley transonic blowdown tunnel.

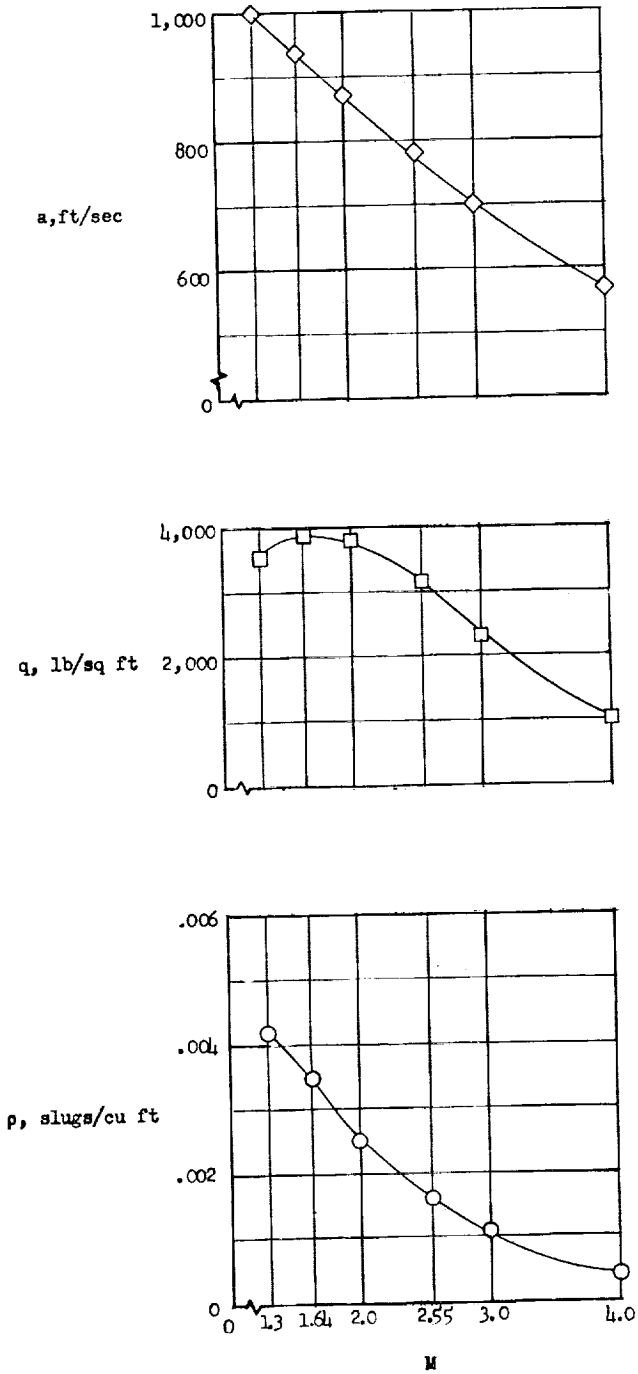

Figure 5.- Performance curves of the Langley 9- by 18-inch supersonic aeroelasticity tunnel showing maximum test-section conditions obtainable.

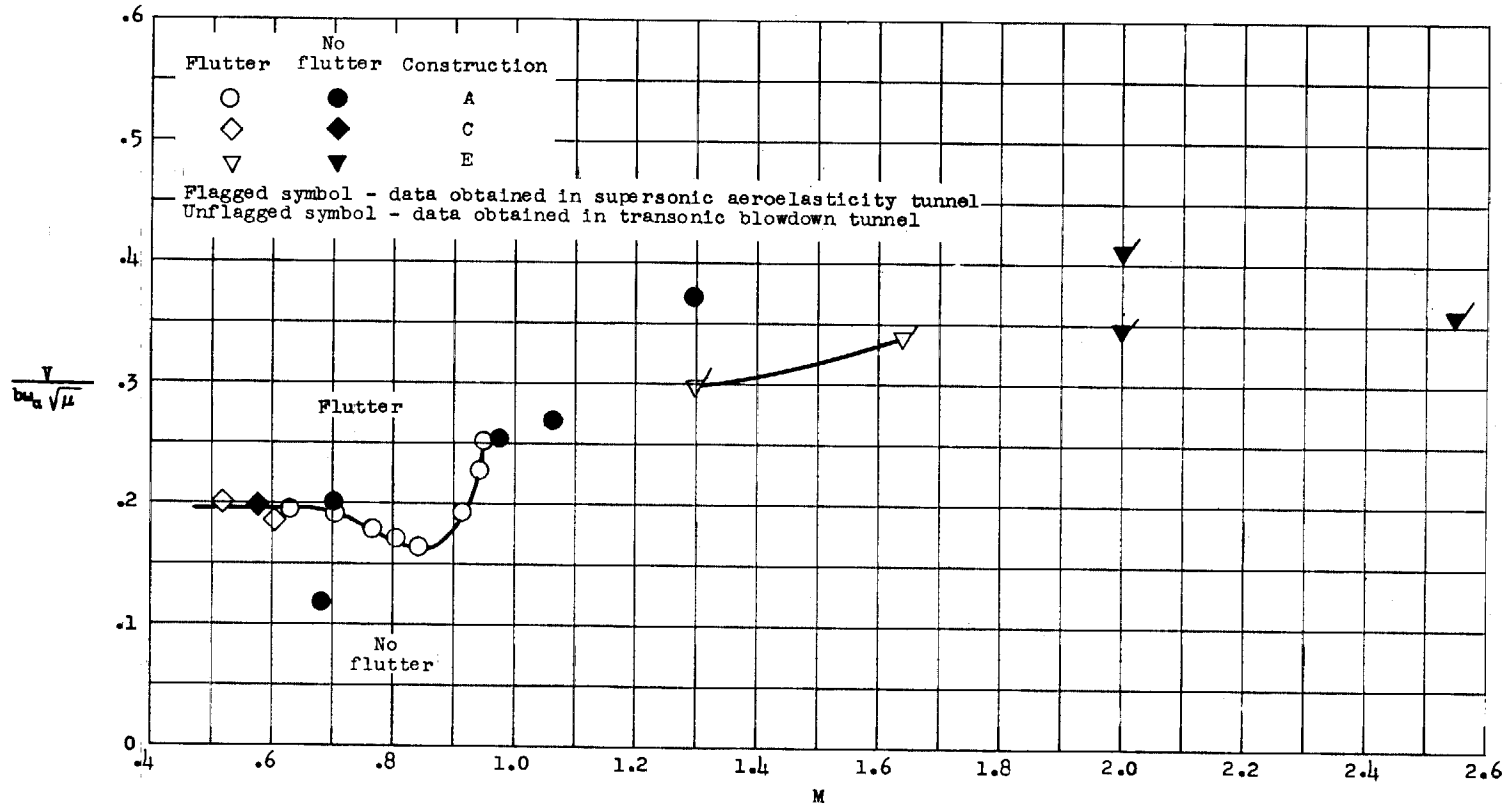

(a) $\Lambda = 25^\circ$.

Figure 6.- Variation of flutter-speed index with Mach number for the three planforms investigated.

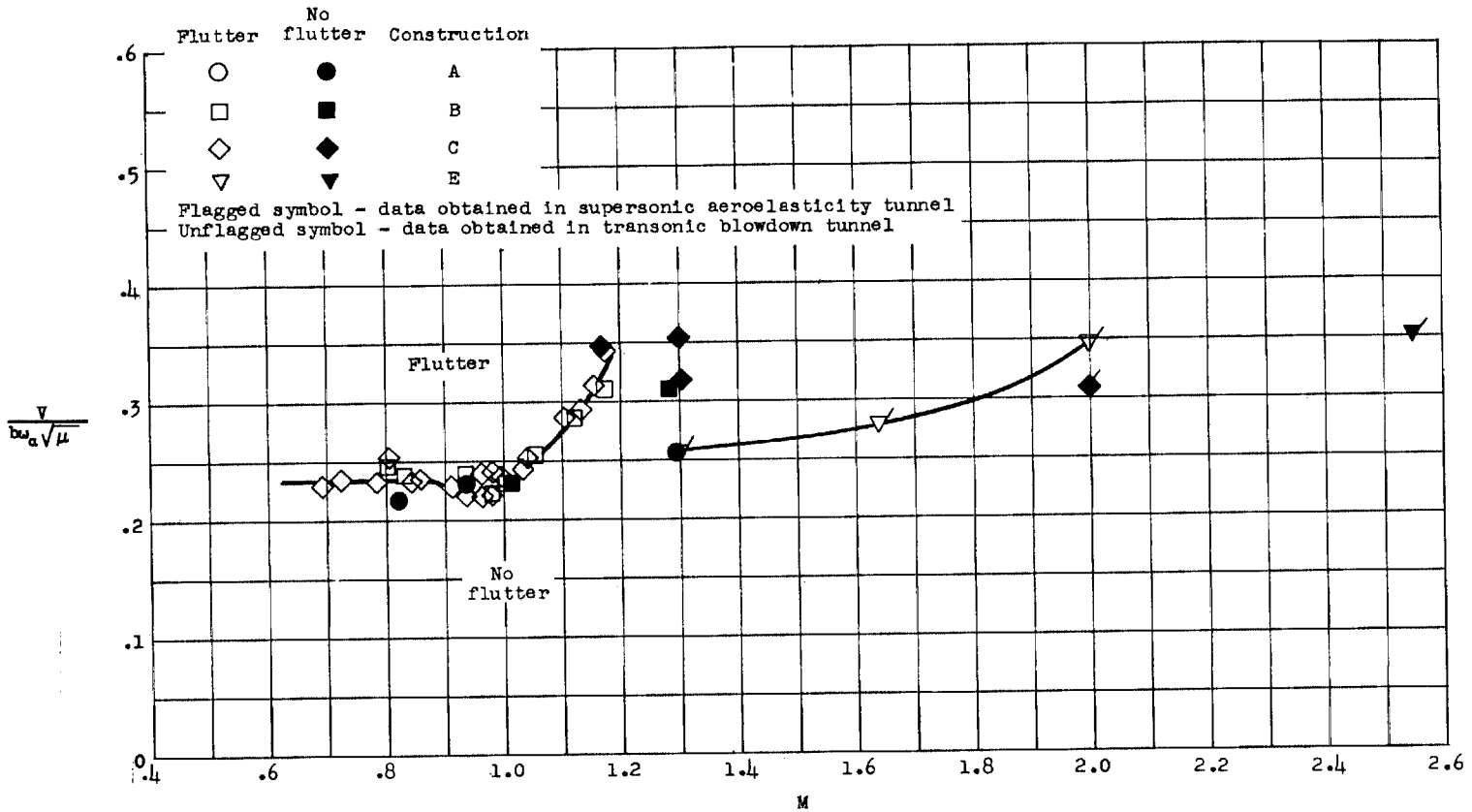

(b) $\Lambda = 60^\circ$.

Figure 6.- Continued.

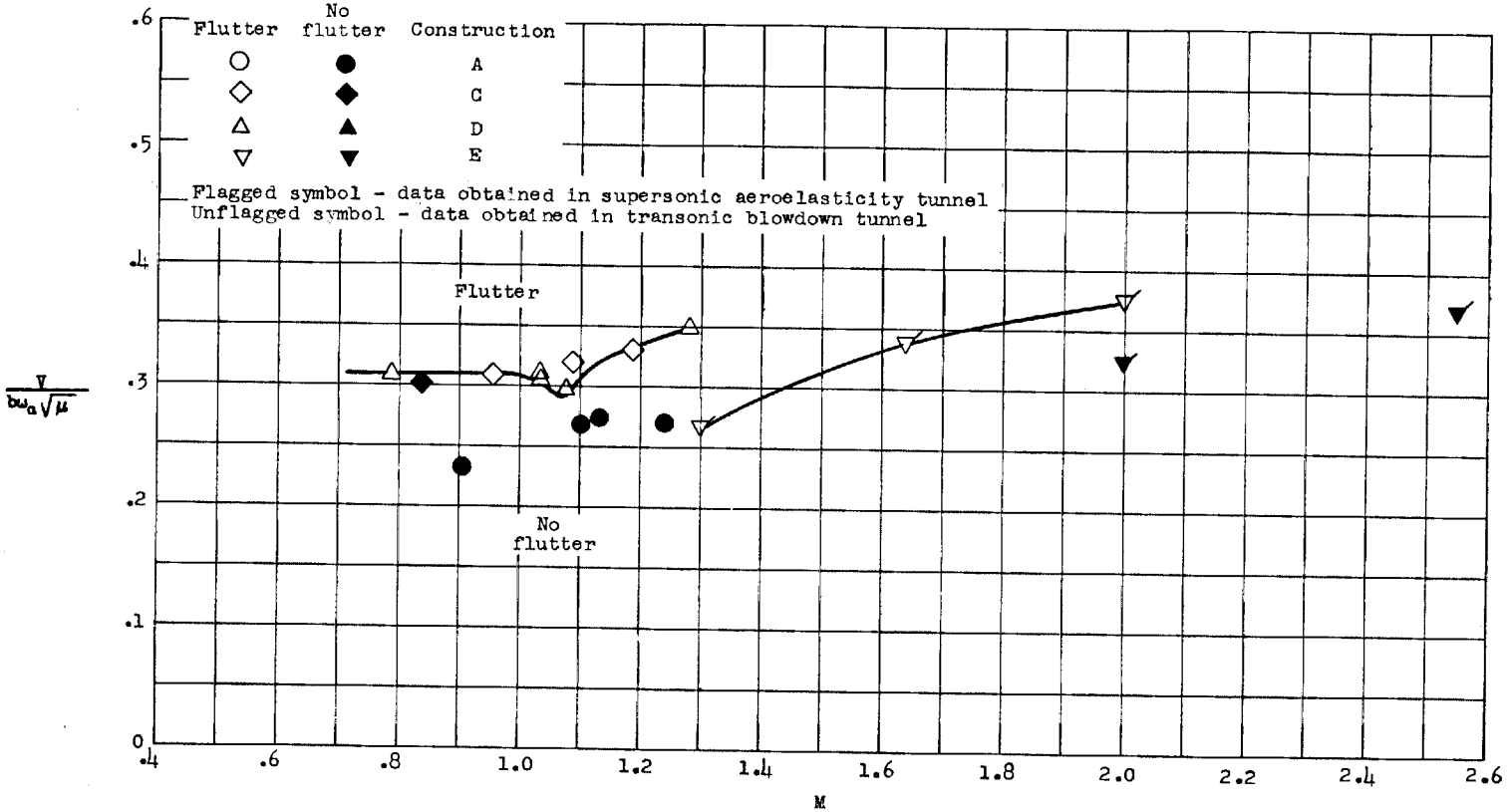

(c) $\Lambda = 75^\circ$.

Figure 6.- Concluded.

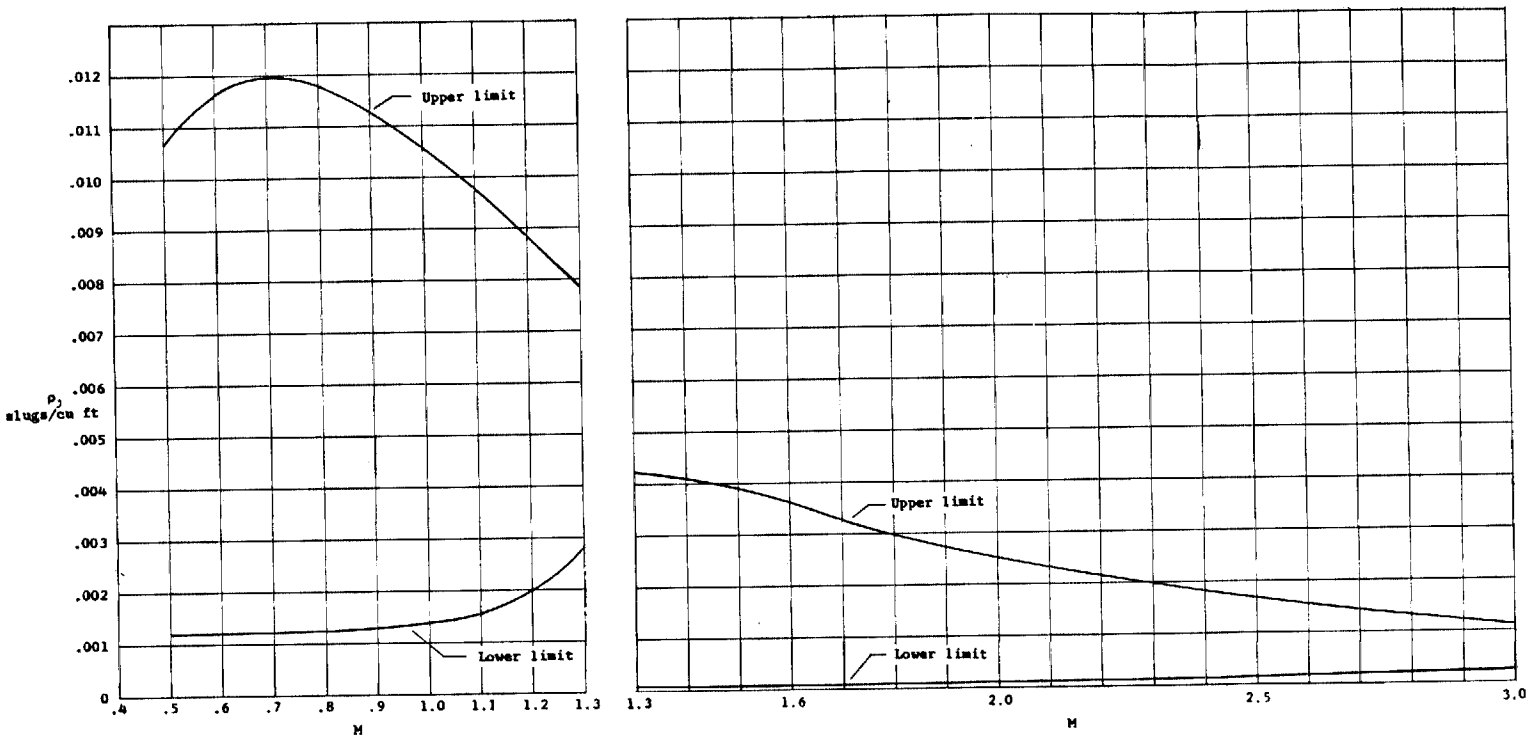

(a) Transonic blowdown tunnel.

(b) Supersonic aeroelasticity tunnel.

Figure 7.- Comparison of density ranges in the Langley transonic blowdown tunnel and the supersonic aeroelasticity tunnel.

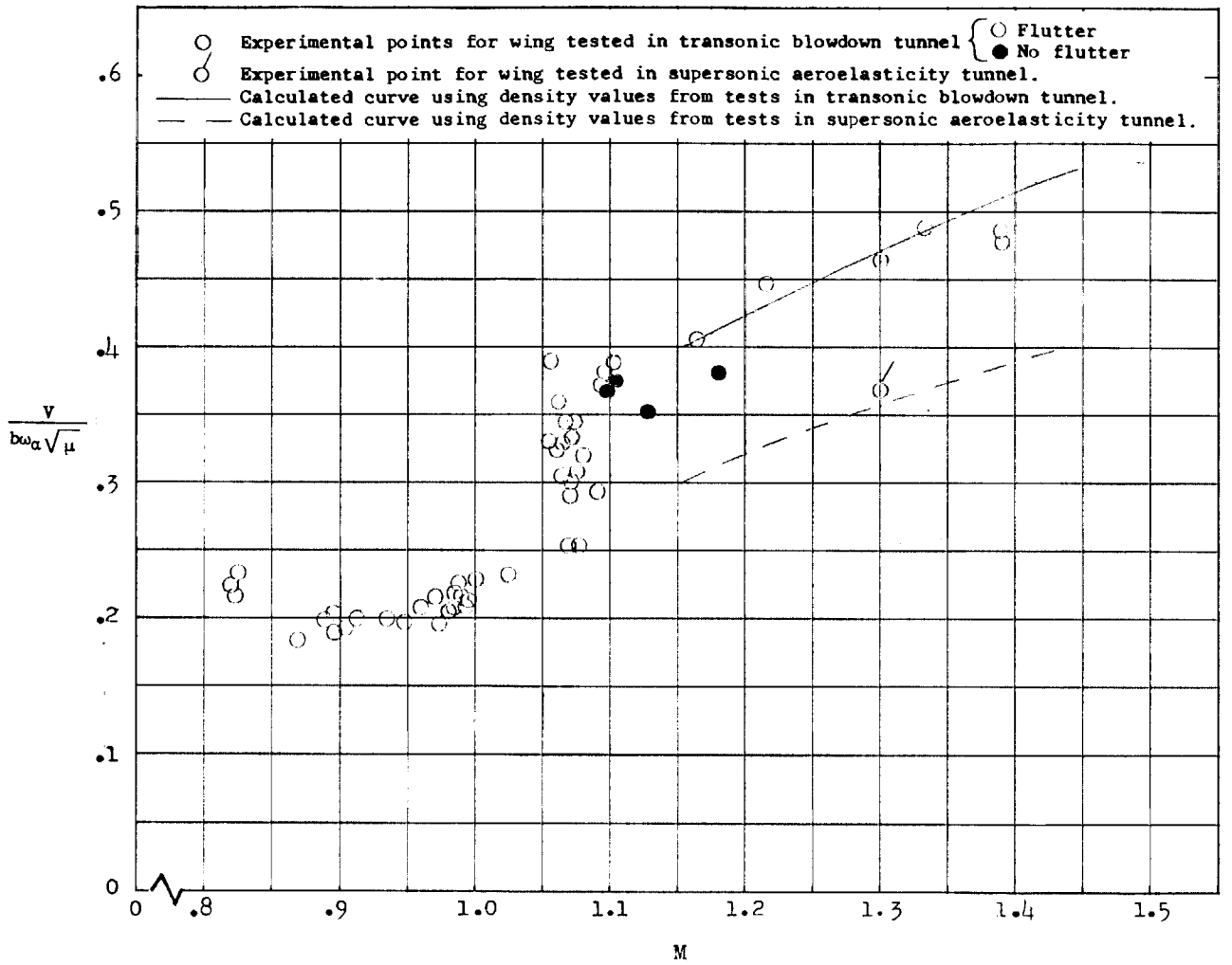

Figure 8.- Comparison of calculated and experimental flutter data for an aspect-ratio-4, taper-ratio-0.2, 45° sweptback wing tested in both the Langley transonic tunnel and the supersonic aeroelasticity tunnel.

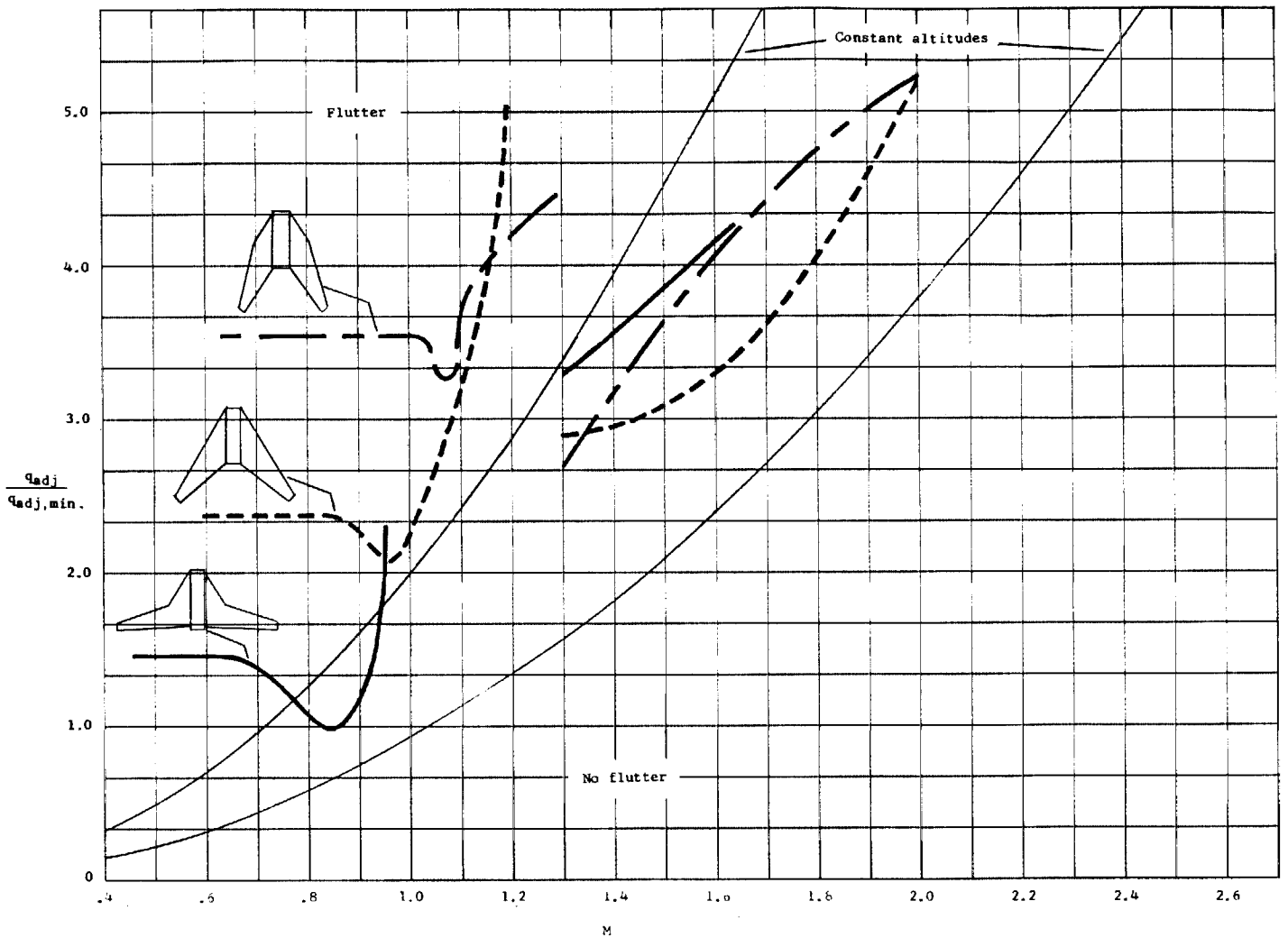

Figure 9.- Flutter boundaries in terms of dynamic pressure applicable to construction A for each planform as a function of Mach number with constant altitudes illustrated.